-Supporting Information-

Removal of antibiotic resistant bacteria and genes by UV-assisted electrochemical oxidation on degenerative TiO_2 nanotube arrays

Siwen Wang [a, b], Shasha Yang [b], Estefanny Quispe [b], Hannah Yang [c], Charles Sanfiorenzo [c], Shane Rogers [b], Kaihang Wang [c], Yang Yang [b, *] and Michael R. Hoffmann [a, *]

[a] Linde+Robinson Laboratories, California Institute of Technology

Pasadena, California 91125 USA

[b] Department of Civil and Environmental Engineering, Clarkson University

Potsdam, New York 13699 USA

[c] Division of Biology and Biological Engineering, California Institute of Technology

Pasadena, California 91125 USA

[*]Corresponding Author:

[a] Phone: +1 626-395-4391; Fax: +1 626-395-2940; E-mail: mrh@caltech.edu

[b] Phone: +1 315-268-3861; Fax: +1 315-268-7985; E-mail: yanyang@clarkson.edu

Submitted to *ACS ES&T Engineering*

February 2021

Text S1. Preparation and Characterization of Blue Nanotube Arrays (BNTA)

The TiO_2 nanotube arrays (NTA) electrode was synthesized by the anodization as reported previously.[1] A 6-cm^2 titanium (Ti) metal plate was coupled with a 6-cm^2 stainless-steel cathode, immersed in an ethylene glycol electrolyte containing 0.25 wt% NH_4F and 2 wt% H_2O. A constant voltage of 40 V was applied between the Ti plate anode and the stainless-steel cathode for 6 h. A layer of NTA film with a thickness of 16 μm grew on the surface of the Ti plate. The NTA electrode was then calcinated at 450°C in air for 1 h to convert the amorphous TiO_2 to the anatase phase. The blue NTA (BNTA) was prepared by applying a cathodic current of 5 mA/cm^2 to the NTA in 15 mM Na_2SO_4 for 5 min.

Text S2. Detailed Methods for Plasmid Construction

The general idea of plasmid construction is to modify the template plasmid, pEB1-sfGFP (kindly provided by Professor Kaihang Wang, Caltech; Addgene plasmid #103983; http://n2t.net/addgene:103983) with the target gene inserts (*i.e.*, *tetA* and *sul1*) which were PCR-amplified from the latrine wastewater, as illustrated in **Figure S1**.

Preparation of the backbone from pEB1-sfGFP with digestion enzyme XbaI.

E. coli MegaX DH10B $T1^R$ Electrocomp cells (Invitrogen by Thermo Fisher Scientific, USA) was used for all the transformation in this study, including the initial propagation of pEB1-sfGFP, construction of all the plasmids. The transformation was carefully prepared following the instruction. The electroporation was performed in a 0.2-cm electroporation cuvette at 2500 V using the Eppendorf Eporator (Eppendorf, Germany). To propagate pEB1-sfGFP, the transformed cells with pEB1-sfGFP was plated on LB agar with 50 μg/mL kanamycin and incubated overnight at 37˚C. Cultures of 100 mL in LB Broth with 50 μg/mL kanamycin were inoculated with single colonies and incubated overnight at 37˚C, 200 rpm. The pEB1-sfGFP were then extracted with a final concentration of ~124 ng/μL by QIAprep Spin Miniprep Kit (Qiagen, USA) following the instruction.

The restriction enzyme XbaI (R0145T, New England Biolabs Inc., USA) was used for the digestion of pEB1-sfGFP to cut off the GFP gene. A total reaction volume of 100 μL was prepared with 10 μL of XbaI, 10 μL of CutSmart Buffer, 40 μL of pEB1-sfGFP stock solution, and 40 μL of nuclease-free water. The digestion reaction was performed overnight at 37˚C. Gel electrophoresis of the digested pEB1-sfGFP was conducted on 1% TBE agarose gels at 100 V for 30 min using Mupid-One Electrophoresis System (Takara Bio Inc., Japan). The bands (**Figure S12**) were visualized by SYBR Safe DNA Gel Stain (10,000X, Thermo Fisher Scientific, USA) with 1 kb plus ladder (New England Biolabs Inc., USA). The gel with the band for the backbone pEB1 (3622 bp) was cut off and purified with GeneJET Gel Extraction Kit (Thermo Fisher Scientific, USA).

Preparation of tetA and sul1 inserts from wastewater.

The two target genes, *tetA* and *sul1*, were first PCR amplified from the latrine wastewater with the primers *tetA*-long and *sul1*-full (**Table S1**). The PCR products were then purified with the QIAquick PCR Purification Kit (QIAGEN, USA). To include an overlap with the backbone pEB1 for assembly, the purified *tetA* and *sul1* genes were then modified with the primers pEB1-tetA and pEB1-sul1 (**Table S1**), respectively, by PCR amplification and then purified with with QIAquick PCR Purification Kit again. The PCR amplification was performed on a Biometra TRIO Thermal Cycler (Analytik Jena, Germany) using PrimeSTAR HS DNA Polymerase (Takara Bio Inc., USA). Each 50 µL PCR reaction contains 10 µL 5X PCR buffer, 4 µL 2.5 mM dNTP, 1 µL of forward and reverse primers at 10 µM, 1 µL template DNA, 0.5 µL PrimeSTAR and 32.5 µL sterilized dH_2O. Thermocycling program was as follows: 98˚C for 1 min followed by 36 cycles of 98˚C for 10 s, annealing temperature (**Table S1**) for 15 s with the primers of *tetA*-long and *sul1*-full or 10 s with longer primers, 72˚C for 1 min, and 72˚C for 30 s after cycles.

Gibson assembly for preparing target plasmids

Then, the complete fragments of *tetA* (1191 bp) and *sul1* (840 bp) were incorporated into backbone pEB1 by Gibson Assembly (Gibson *et al.*, 2009) forming the resulting plasmids pEB1-tetA and pEB1-sul1, respectively (shown in **Figure S1**).

Functionality analysis and structural sequencing for constructed plasmids

The plasmids were then transformed into DH10B and then plated on LB agar with 50 µg/mL Kanamycin and incubated overnight at 37˚C. Twenty-three colonies were picked from the plates for each cloned plasmid and suspended in 40 µL dH_2O. The culture suspension of DH10B transformed with pEB1-sfGFP was also prepared as negative control. Then 5 µL of each culture suspension was stamped on plain LB agar and LB agar with 10 µg/mL tetracycline for pEB1-tetA or LB agar with 200 µg/L sulfamethoxazole for pEB1-sul1. Two randomly selected positive colonies stamped on selective LB agar plate for each cloned plasmid are shown in **Figure S13**.

The two colonies were inoculated in selected LB media and grown overnight at 37˚C, 200 rpm. Plasmids were extracted from the culture and subsequently sequenced using Sanger sequencing (Laragen Sequencing and Genotyping, USA). For the target plasmid pEB1-tetA, 4 primers (pEB1-Bb-FW, pEB1-Bb-RV, *tetA*-long-FW, and *tetA*-short-RV, shown in **Table S1**) were used for

sequencing. A sequence length of 1420 bp (including 181 bp before *tetA*, the first 528 bp of *tetA*, the last 592 bp of *tetA*, and 49 bp after *tetA*) was aligned using SnapGene (USA) and 8 base pair mutations resulting in 3 amino acid mutations that were observed; all occurred in the *tetA* gene. The positions of the mutations are listed in **Table S5** and shown in **Figure S14**. Since the similarity of the aligned sequence is 99.5% and the tetracycline-resistance was successfully expressed by DH10B cells, we kept the gene as *tetA* in this study. For the target plasmid pEB1-sul1, 4 primers (pEB1-Bb-FW, pEB1-Bb-RV, *sul1*-full-FW and *sul1*-full-RV, shown in **Table S1**) were used for sequencing. A sequence length of 1105 bp (including the complete 840 bp of *sul1* gene with 198 bp before and 67 bp after *sul1*) were aligned using SnapGene (USA), and no mismatch was found (100% similarity). The maps of the two constructed plasmids were generated using Snapgene Software (Version 5.2.0, GSL Biotech LLC) and are shown in **Figure S2**.

Plasmid extraction

The transformed DH10B culture with the cloned pEB1-tetA or pEB1-sul1 was stored at -80˚C in 15% glycerol as stock. All the cell cultures thereafter were cultivated directly from the stocks in LB Broth with 10 µg/mL tetracycline or 200 µg/mL SMX at 37˚C, 200 rpm overnight. To prepare plasmid stocks, several extractions were conducted for both pEB1-tetA and pEBA-sul1. The concentrations of the plasmid DNA in the plasmid stocks are 80-170 ng/µL as measured a Nanodrop One C (Thermo Fisher Scientific, USA).

Text S3. Effect of electrolytes on the DNA analysis by gel electrophoresis and qPCR inhibition.

The effect of the electrolytes on gel electrophoresis and qPCR inhibition was investigated. The background electrolyte, NaCl, at an initial concentration of 30 mM was electrolyzed under a constant direct current of 30 mA with UV radiation for 0 s, 1 min, 5 min, and 10 min. Then the stock samples of pEB1-sul1 and purified PCR amplicon of *sul1* (840 bp) were spiked into the electrolyzed NaCl with varied electrolysis durations. They were then analyzed by gel electrophoresis and qPCR measurement. No differences were observed in the gel electrophoresis results (**Figure S3**) or qPCR (**Figure S4**) between the samples taken during the zero applied potential electrolysis (*i.e.*, no electrolysis) experiments and electrolyzed NaCl.

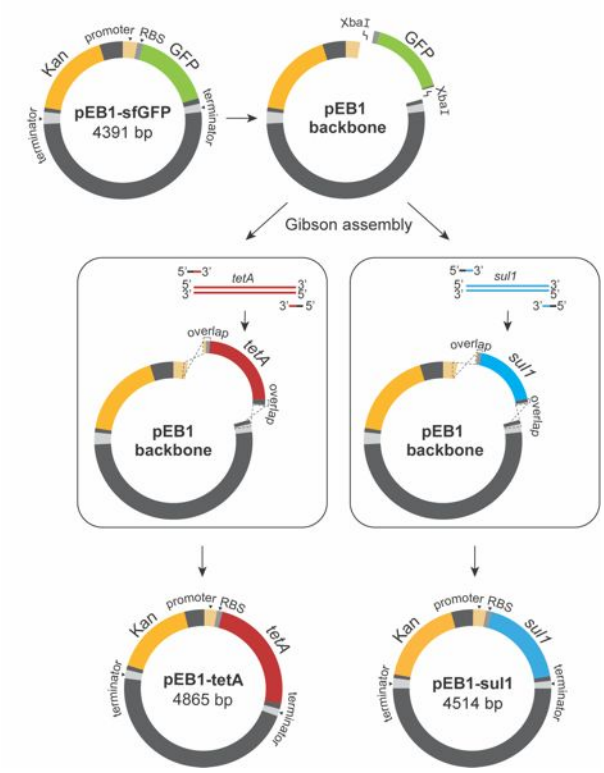

Figure S1. Plasmid construction performed for pEB1-tetA and pEB1-sul1.

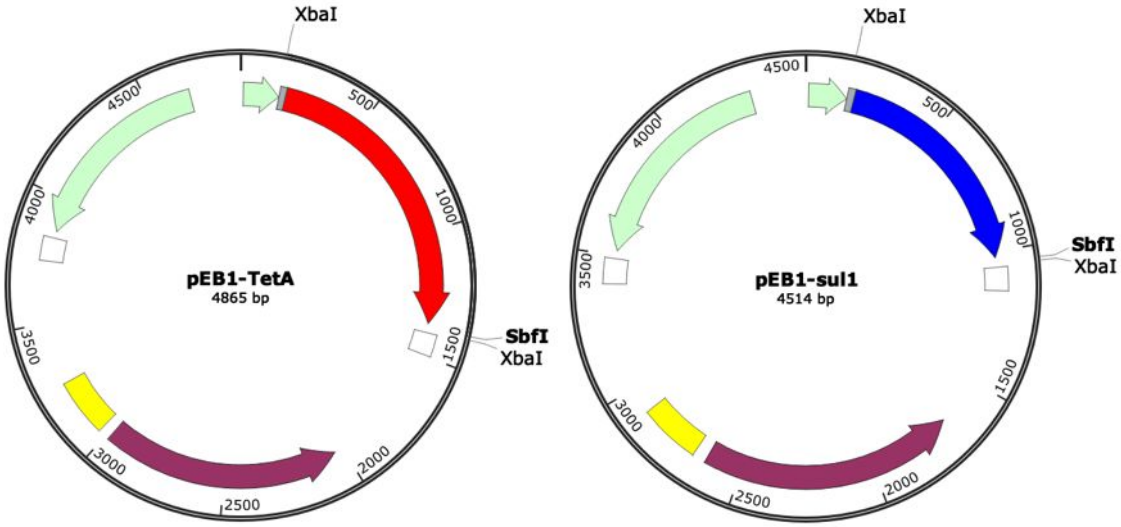

Figure S2. Plasmid DNA maps of pEB1-tetA and pEB1-sul1, showing the positions of two restriction enzymes, XbaI and SbfI.

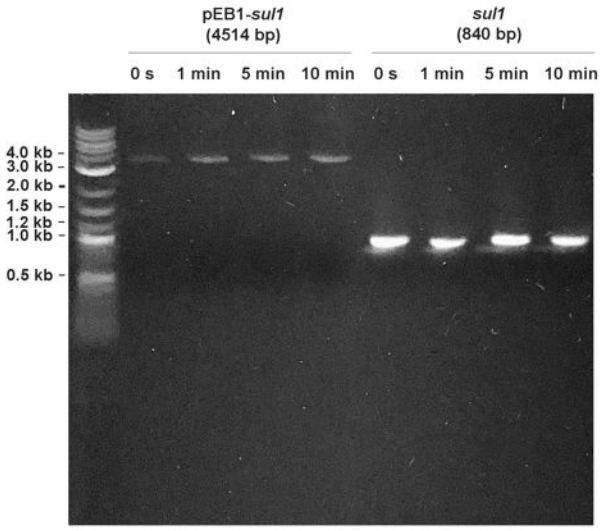

Figure S3. Gel electrophoresis of pEB1-sul1 and *sul1* spiked in electrolyzed NaCl (30 mM) with different electrolysis durations.

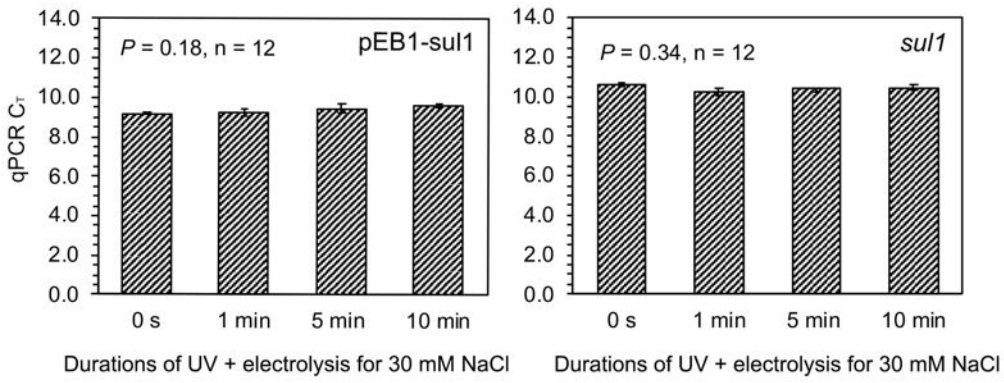

Figure S4. C_T values (*sul1*_long) of spiked pEB1-sul1 and *sul1* as a function of variable durations for UV-EO treated NaCl with an initial concentration of 30 mM. No difference was observed between the samples in untreated and treated NaCl with *P* values of 0.18 and 0.34 for pEB1-sul1 and *sul1*, respectively (ANOVA test).

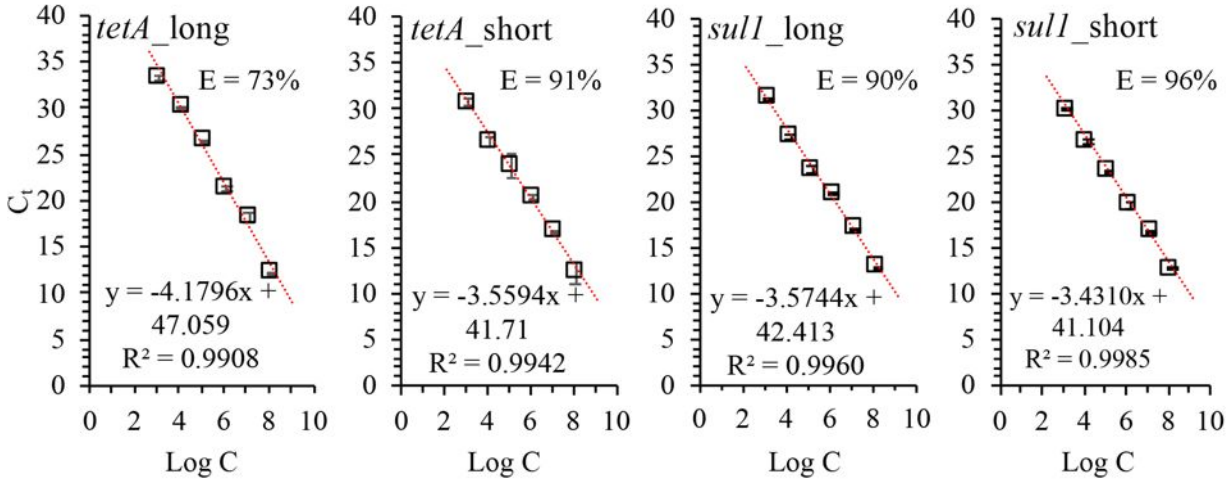

Figure S5. The qPCR calibration curves for 4 amplicons, *tetA*_long (1200 bp), *tetA*_short (216 bp), *sul1*_long (827 bp) and *sul1*_short (162 bp), with slope, y-intercept, R^2 and PCR efficiency (E) calculated from $10^{(-1/slope)}$-1. The error bars represent one-standard deviation of triplicate measurements.

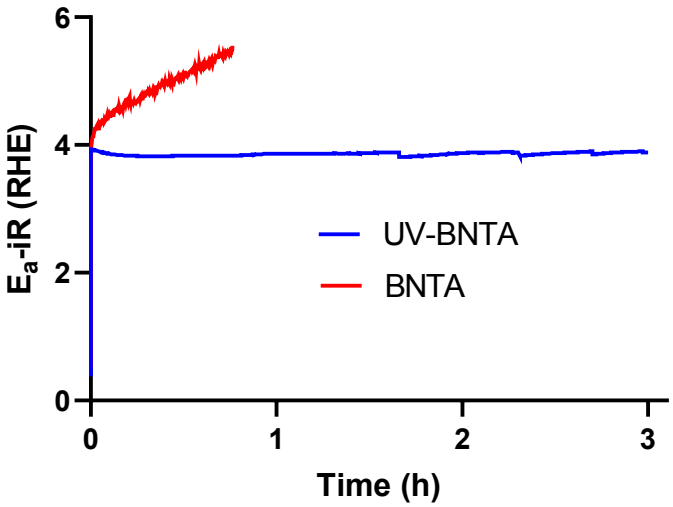

Figure S6. Stability tests on BNTA anode performed in 15 mM Na_2SO_4 at 10 mA/cm^2 in the presence and absence of UV irradiation.

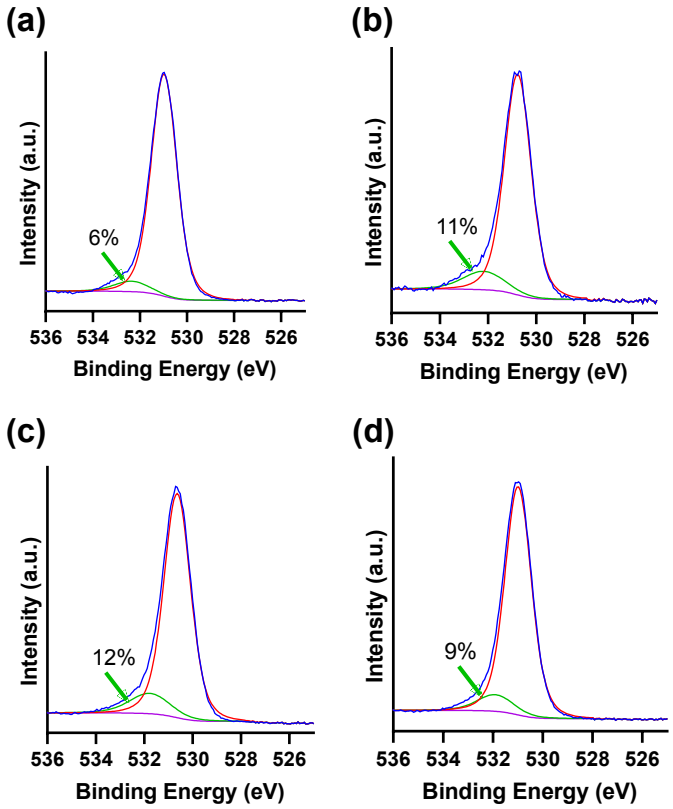

Figure S7. O1s XPS orbitals of (a) NTA, (b) BNTA, (c) BNTA after 1 h electrolysis with UV_{254} irradiation, and (d) BNTA after 1 h electrolysis without UV_{254} irradiation. The peak of O1s orbital can be deconvoluted to a main peak centered at 531 eV and shoulder peak centered at 532 eV. The former can be assigned to fully coordinated lattice oxygen (O_{lat}), while the latter corresponds to oxygen vacancies (O_{vac}).[2,3] It is important to note that XPS analysis gives semi-qualitative comparison rather than qualitative numbers and that uncertainties lie in the peak deconvolution even if the FWHM of O_{lat} and O_{vac} are set as the same. More precise crystal structure characterizations performed on synchrotron X-ray absorption spectroscopy are underway.

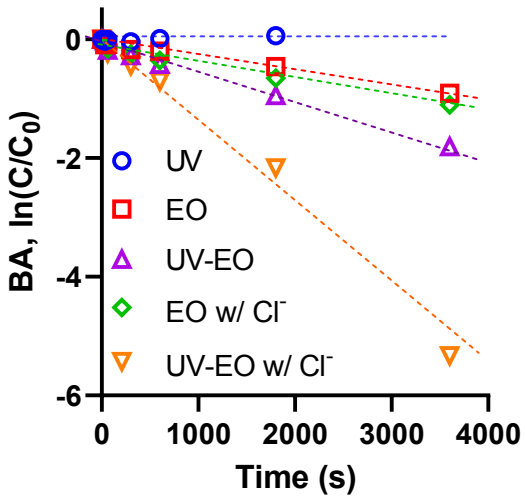

Figure S8. BA degradation by BNTA at 10 mA/cm^2 in the absence (EO) and presence (UV-EO) of UV. All the test was performed in 30 mM $NaClO_4$ except tests "EO w/ Cl^-" and "UV-EO w/ Cl^-" were conducted in 30 mM NaCl. Experimental data were fitted by the first-order kinetics.

It is assumed that the intrinsic reaction between BA and ·OH follows second-order kinetics, which can be further simplified to a form of pseudo-order kinetics as **Eq. S1**:

$$\frac{dC_{\mathrm{BA}}}{dt} = k_{\cdot OH}[\cdot \mathrm{OH}][\mathrm{BA}] = k_{obs}[\mathrm{BA}] \qquad \textbf{(Eq. S1)}$$

The observed rate constant (k_{obs}) fitted by linear regression is 2.58 × 10^{-4} s^{-1}. The corresponding steady-state ·OH concentration ($[\cdot \mathrm{OH}]_{\mathrm{ss}}$) is calculated to be 4.37 × 10^{-14} M according to **Eq. S2**.

$$[\cdot \mathrm{OH}]_{ss} = \frac{k_{obs}}{k_{\cdot OH}} \qquad \textbf{(Eq. S2)}$$

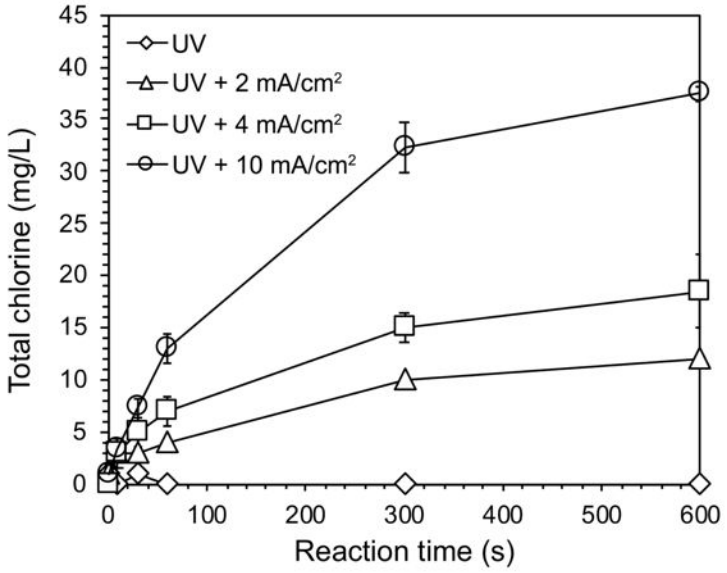

Figure S9. Chlorine evolution during UV-EO process in 30 mM NaCl at varied current densities. Error bars represent one standard deviation from triplicate experiments.

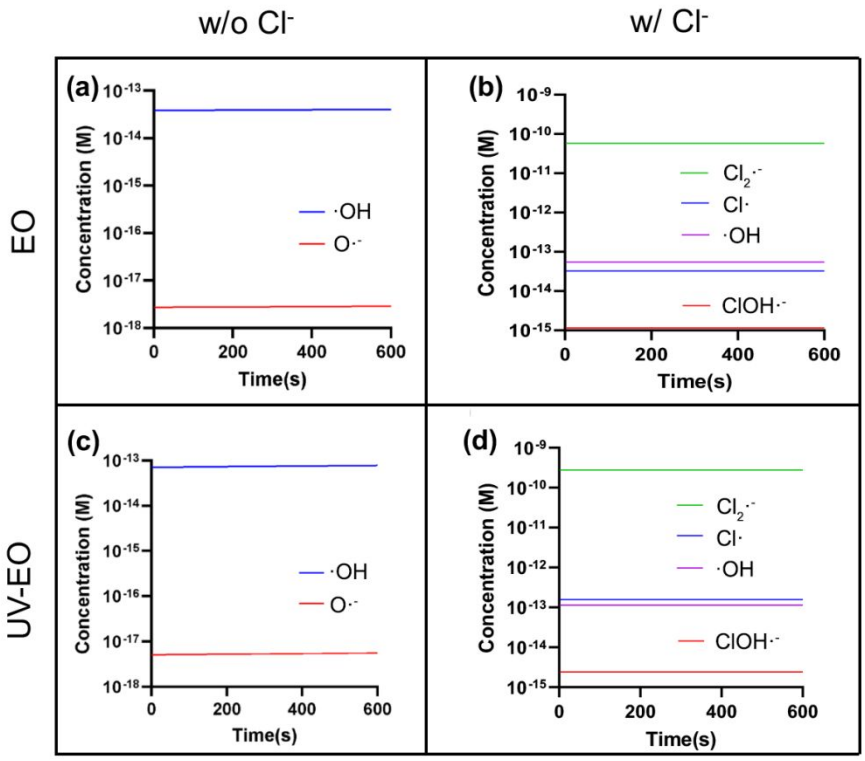

Figure S10. Radical speciation estimated by the kinetic model developed in this study, with the conditions: (a) EO w/o Cl^-, (b) EO w/Cl^-, (c) UV-EO w/o Cl^-, and (d) UV-EO w/Cl^- in the presence of 30 mM NaCl and 35 mg/L free chlorine.

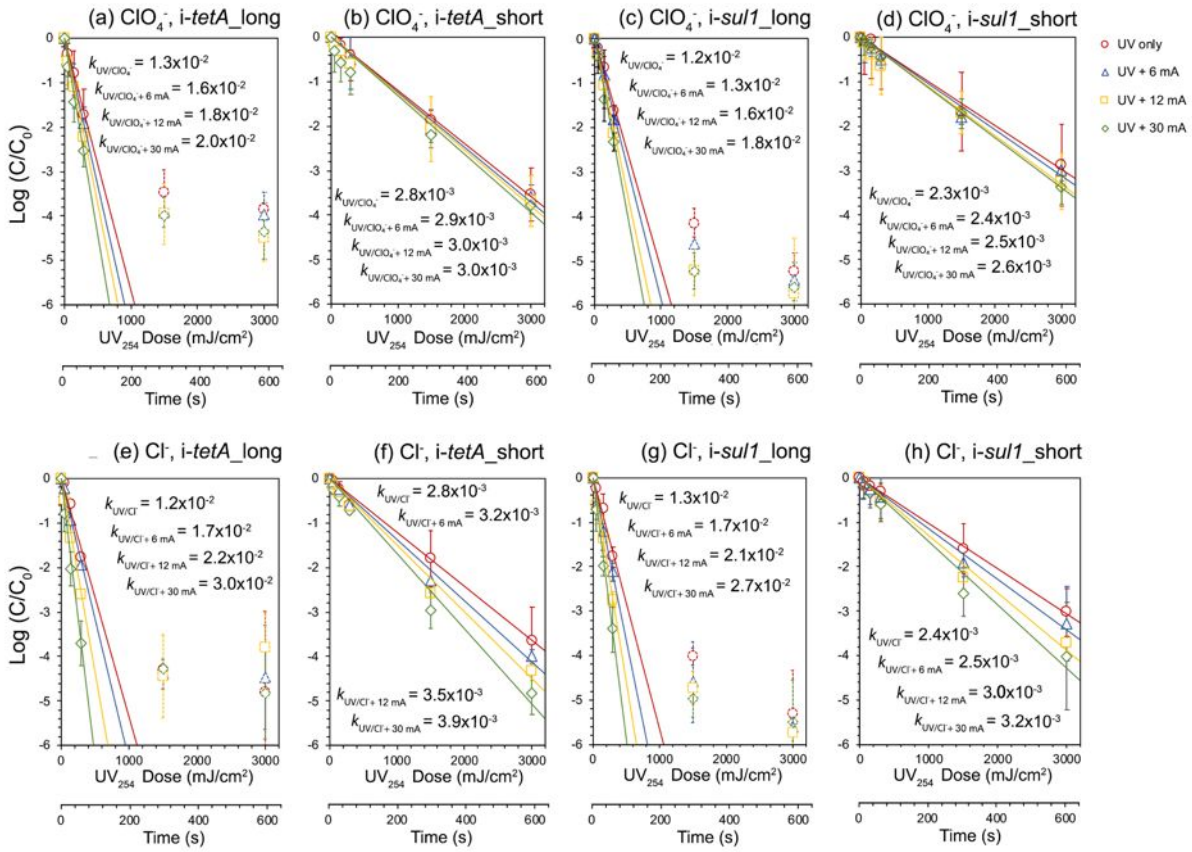

Figure S11. Logarithmic relative concentrations of both long and short qPCR amplicons for *tetA* and *sul1* as a function of 1) UV_{254} dose and 2) time, during treatment of intracellular plasmids hosted in *E. coli* DH10B with UV_{254} irradiation alone and UV-EO at various currents conducted in 30 mM $NaClO_4$ (a-d) and 30 mM NaCl (e-h). The error bars represent standard deviation from triplicate experiments and the lines represent the linear regressions of the data. The fluence-based first-order kinetics rates *k* are derived from the slope of the linear curves and labeled in unit of cm^2/mJ. Some data points are excluded from linear regression due to their deviation from first-order kinetics by observation and labeled in the dashed border.

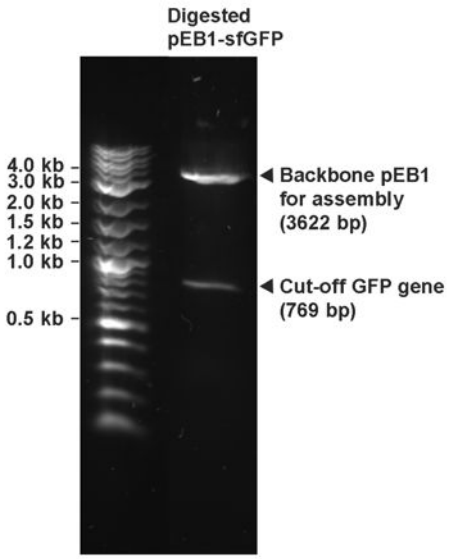

Figure S12. DNA gel electrophoresis of pEB1-sfGFP after digestion by XbaI.

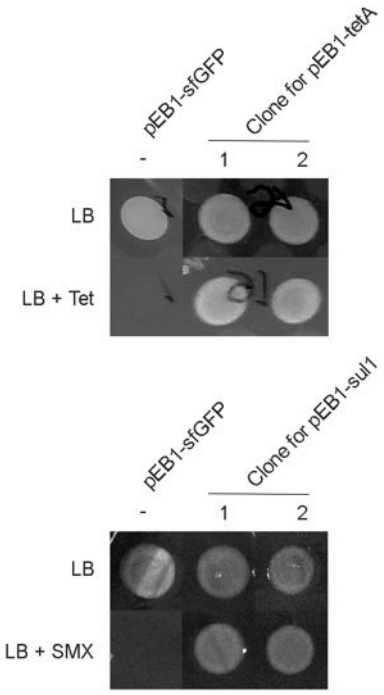

Figure S13. Growth of DH10B transformed by pEB1-sfGFP (-) and by the cloned pEB1-tetA and pEB1-sul1 (Tet, teracycline; SMX, sulfamethoxazole).

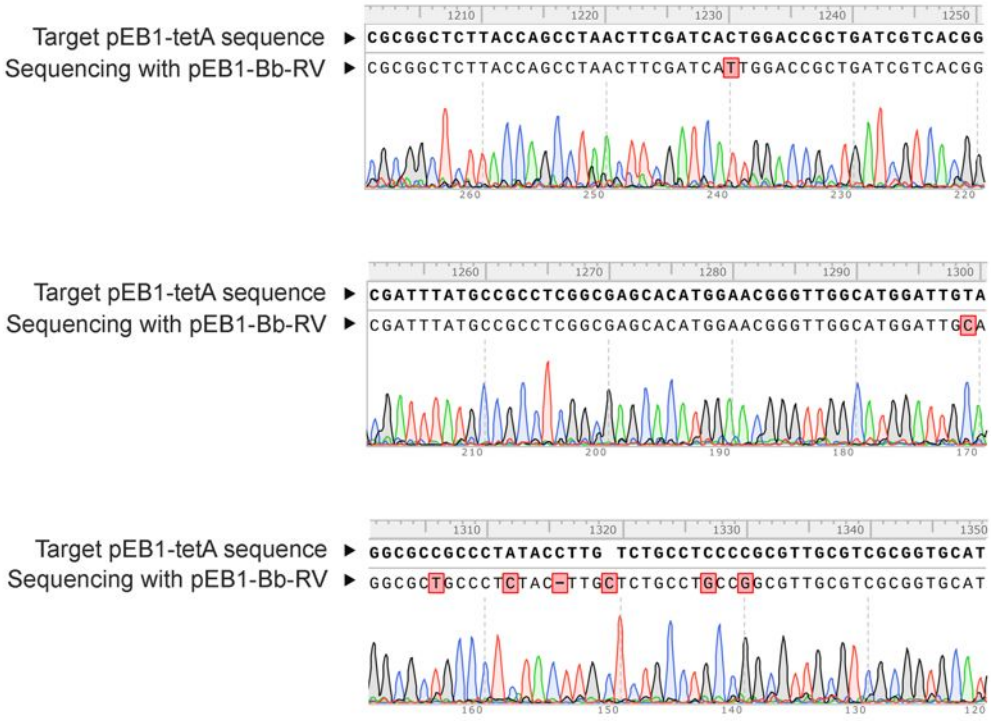

Figure S14. Chromatogram of Sanger sequencing for cloned pEB1-tetA with annotated mutations.

Table S1. List of primers used in this study.

Primer	Sequence (5'-3')		Oligo size (nt)	Annealing temperature (°C)	Amplicon size (bp)	Annotation	Reference
tetA-long	FW:	CGT GTA TGA AAT CTA ACA ATG CGC T	25	51.9	1200	For qPCR quantification of *tetA* long amplicon, amplifying full-length tetA gene from wastewater, and sanger sequencing to check on the constructed plasmid	Chang *et al.*, 2017 [7]
	RV:	CCA TTC AGG TCG AGG TGG C	19				
tetA-short	FW:	GAC TAT CGT CGC CGC ACT TA	20	53.9	216	For qPCR quantification of *tetA* short amplicon	Chang *et al.*, 2017 [7]
	RV:	ATA ATG GCC TGC TTC TCG CC	20				
sul1-long	FW:	GAC GGT GTT CGG CAT TCT	18	60	827	For qPCR quantification of *sul1* long amplicon	Czekalski *et al.*, 2016 [8]
	RV:	GAT CTA ACC CTC GGT CTC TGG	21				
sul1-short	FW:	CGC ACC GGA AAC ATC GCT GCA C	22	60	162	For qPCR quantification of *sul1* short amplicon	Xu *et al.*, 2015 [9]
	RV:	TGA AGT TCC GCC GCA AGG CTC G	22				
sul1-full	FW:	ATG GTG ACG GTG TTC GGC ATT CTG AAT CT	29	60	840	For amplifying full-length sul1 gene from wastewater and sanger sequencing to check on the constructed plasmid	this study
	RV:	CTA GGC ATG ATC TAA CCC TCG GTC TCT GGC	30				
pEB1-Bb-tetA	FW:	TCT ACA AAT AAT TTT GTT TAA CTT TTC TAG ATT TAA GAA GGA GAT ATA CAT ATG AAA TCT AAC AAT GCG CTC ATC GTC	87	60.0	1294	For adding an overlap of pEB1 backbone on each end of tetA genes	this study

		ATC CTC GGC					
	RV:	CTT TCG TTT TAT TTG ATG CCT CTA GAG CTT GCA TGC CTG CAG GTC TGG ACA TTC AGG TCG AGG TGG CCC GGC TCC ATG	78				
pEB1-Bb-sul1	FW:	TCT ACA AAT AAT TTT GTT TAA CTT TTC TAG ATT TAA GAA GGA GAT ATA CAT ATG GTG ACG GTG TTC GGC ATT CTG AAT CT	80	60	942	For adding an overlap of pEB1 backbone on each end of sul1 genes	this study
	RV:	TTT CGT TTT ATT TGA TGC CTC TAG AGC TTG CAT GCC TGC AGG TCT GGA CAT CTA GGC ATG ATC TAA CCC TCG GTC TCT GGC	81				
pEB1-Bb	FW:	TTT GCA GGG CTT CCC AAC CTT ACC AGA GGG	30	65	1261	For sanger sequencing to check on the constructed plasmid	this study
	RV:	CGG ATT TGT CCT ACT CAG GAG AGC GTT CA	29				

Table S2. Wastewater conditions before and after the UV-EO treatment by BNTA at 30 mA for 30 min.

	Before treatment	After treatment
NH_3-N (mg/L)	445	390
COD (mg/L)	236	174
pH	9.0	8.9
Total chlorine (mg/L)	0.0	4.0
Conductivity (mS/cm)	5.0	

Table S3. Critical reactions included in the kinetic model.

Reaction No.	Reaction	Rate constant	Reference
pH-dependent equilibrium			
1	$H^+ + OH^- \rightarrow H_2O$	1.00×10^{11} M^{-1} s^{-1}	16
2	$H_2O \rightarrow H^+ + OH^-$	1.00×10^{-3} M^{-1} s^{-1}	16
3	$OCl^- + H^+ \rightarrow HOCl$	5.00×10^{10} M^{-1} s^{-1}	16
4	$HOCl \rightarrow OCl^- + H^+$	1.60×10^{3} M^{-1} s^{-1}	16
Electrochemical reactions			
5*	$M\text{-}OH \rightarrow HO^{\cdot}$	EO: 6.1×10^{-7} M s^{-1} UV-EO: 1.1×10^{-6} M s^{-1}	Fitted value
6*	$MO + Cl^- \rightarrow Cl^{\cdot}$	8.8×10^{-5} s^{-1}	Fitted value
UV/chlorine			
7	$HOCl \rightarrow Cl^{\cdot} + HO^{\cdot}$	3×10^{-4} M s^{-1}	Fitted value
$Cl^{\cdot}$ generation			
8	$Cl^- + HO^{\cdot} \rightarrow ClOH^{\cdot}$	4.30×10^{9} M^{-1} s^{-1}	17
9	$ClOH^{\cdot} \rightarrow Cl^- + HO^{\cdot}$	6.10×10^{9} M^{-1} s^{-1}	18
10	$Cl^{\cdot} + OH^- \rightarrow ClOH^{\cdot -}$	1.80×10^{10} M^{-1} s^{-1}	19
11	$ClOH^{\cdot -} + H^+ \rightarrow Cl^{\cdot} + H_2O$	2.10×10^{10} M^{-1} s^{-1}	18
12	$ClOH^{\cdot -} + Cl^- \rightarrow Cl_2^{\cdot -} + OH^-$	1.00×10^{5} M^{-1} s^{-1}	20
13	$Cl_2^{\cdot -} + OH^- \rightarrow ClOH^{\cdot -} + Cl^-$	4.50×10^{7} M^{-1} s^{-1}	20
14	$Cl^{\cdot} + Cl^- \rightarrow Cl_2^{\cdot -}$	6.50×10^{9} M^{-1} s^{-1}	19
15	$Cl_2^{\cdot -} \rightarrow Cl^{\cdot} + Cl^-$	1.10×10^{5} M^{-1} s^{-1}	18
Cl_2 generation			
16	$Cl^{\cdot} + Cl^{\cdot} \rightarrow Cl_2$	1.00×10^{8} M^{-1} s^{-1}	21
17	$Cl^{\cdot} + Cl_2^{\cdot -} \rightarrow Cl^- + Cl_2$	1.40×10^{9} M^{-1} s^{-1}	22
18	$Cl_2^{\cdot -} + Cl_2^{\cdot -} \rightarrow 2Cl^- + Cl_2$	8.30×10^{8} M^{-1} s^{-1}	17
19	$Cl_2^{\cdot -} + HO^{\cdot} \rightarrow HOCl + Cl^-$	1.00×10^{9} M^{-1} s^{-1}	17
Cl_2 dissolution			
20	$Cl_2 + H_2O \rightarrow Cl_2OH^- + H^+$	1.50×10^{1} M^{-1} s^{-1}	23
21	$Cl_2OH^- \rightarrow HOCl + Cl^-$	5.50×10^{9} M^{-1} s^{-1}	23
$HO^{\cdot}$ transformation			
22	$HO^{\cdot} \rightarrow O^{\cdot -} + H^+$	1.26×10^{12} M^{-1} s^{-1}	24
23	$O^{\cdot -} + H_2O \rightarrow HO^{\cdot} + OH^-$	1.80×10^{6} M^{-1} s^{-1}	24
24	$HO^{\cdot} + OH^- \rightarrow O^{\cdot -} + H_2O$	1.30×10^{10} M^{-1} s^{-1}	
HO_2^-, $HO_2^{\cdot}$, $O_2^{\cdot -}$ related			
25	$HO^{\cdot} + O^{\cdot -} \rightarrow HO_2^-$	1.00×10^{10} M^{-1} s^{-1}	24
26	$HO^{\cdot} + HO_2^- \rightarrow HO_2^{\cdot} + OH^-$	7.50×10^{9} M^{-1} s^{-1}	24
27	$HO_2^{\cdot} + O_2^{\cdot -} \rightarrow HO_2^- + O_2$	9.70×10^{7} M^{-1} s^{-1}	24
28	$HO^{\cdot} + HO_2^{\cdot} \rightarrow H_2O + O_2$	6.60×10^{9} M^{-1} s^{-1}	24
29	$HO_2^{\cdot} + HO_2^{\cdot} \rightarrow H_2O_2 + O_2$	8.30×10^{5} M^{-1} s^{-1}	24
30	$HO_2^{\cdot} \rightarrow H^+ + O_2^{\cdot -}$	1.60×10^{5} M^{-1} s^{-1}	25
31	$HO^{\cdot} + O_2^{\cdot -} \rightarrow OH^- + O_2$	8.00×10^{9} M^{-1} s^{-1}	24
Radicals quenched by free chlorine			
32	$HO^{\cdot} + HOCl \rightarrow ClO^{\cdot} + H2O$	2.00×10^{9} M^{-1} s^{-1}	16
33	$HO^{\cdot} + OCl^- \rightarrow ClO^{\cdot} + OH^-$	8.80×10^{9} M^{-1} s^{-1}	
34	$Cl^{\cdot} + HOCl \rightarrow ClO^{\cdot} + H^+ + Cl^-$	3.00×10^{9} M^{-1} s^{-1}	27
35	$Cl^{\cdot} + OCl^- \rightarrow ClO^{\cdot} + Cl^-$	8.20×10^{9} M^{-1} s^{-1}	18
Radicals quenched by benzoic acid			

36	$HO^{\cdot} + C_6H_5COO^{-} \rightarrow$ Products	5.90×10^9 M^{-1} s^{-1}	[24]
37	$Cl^{\cdot} + C_6H_5COO^{-} \rightarrow$ Products	1.80×10^{10} M^{-1} s^{-1}	[28]
38	$Cl_2^{\cdot -} + C_6H_5COO^{-} \rightarrow$ Products	2.00×10^6 M^{-1} s^{-1}	[29]
39	$O^{\cdot -} + C_6H_5COO^{-} \rightarrow$ Products	4.00×10^7 M^{-1} s^{-1}	[24]

* The M-OH and MO represents the active sites of BNTA to generate ·OH radicals and oxidize Cl^-, respectively. The active sites are assumed to be infinite. Thus, {M-OH} and {MO} were set as one in the model. The reactions then follow zero-order kinetics.

Table S4. Summary of kinetic parameters for ARB inactivation and ARG degradation/deactivation from literature and this study (UV alone and UV combined with H_2O_2 or Chlorine).

Gene	Gene length (bp)	DNA type	DNA name	DNA location	DNA length (bp)	Hteost cell	Inactivation type	Initial DNA/ cell concentration	Amplicon length (bp)	Reagent for treatment	Kinetic rates (cm^2/mJ for UV; M^{-1} s^{-1} for H_2O_2; L/(mg•min) for chlorine)	Regression model	* Required dose for 2-log_{10} reduction (mJ/cm^2 for UV; M・s for H_2O_2; mg/L•min for chlorine)	* Required dose for 4-log_{10} reduction (mJ/cm^2 for UV; M・s for H_2O_2; mg/L•min for chlorine)	Reference
UV_{254}															
tetA	1191	plasmid	pEB1-tetA		4865	*E. coli* DH10B	culturability (selective agar)	~2.3×10^7 CFU/mL		30 mM $NaClO_4$		fluence-based first order		50 (3.9 log10)	This study
sul1	840	plasmid	pEB1-sul1		4514	*E. coli* DH10B	culturability (selective agar)	~2.8×10^7 CFU/mL		30 mM $NaClO_4$		fluence-based first order	50 (2.6-log_{10})	150 (4.2 log10)	
tetA	1191	plasmid	pEB1-tetA	intracellular	4865	*E. coli* DH10B	gene damage (by qPCR)	~2.3×10^7 CFU/mL	1200	30 mM $NaClO_4$	$1.3 (\pm 0.10)\times10^{-2}$	fluence-based first order	354	>3000	
tetA	1191	plasmid	pEB1-tetA	intracellular	4865	*E. coli* DH10B	gene damage (by qPCR)	~2.3×10^7 CFU/mL	216	30 mM $NaClO_4$	$2.8 (\pm 0.03)\times10^{-3}$	fluence-based first order	1645	>3000	
tetA	1191	plasmid	pEB1-tetA	extracellular	4865	*E. coli* DH10B	gene damage (by qPCR)	8×10^8 copies/µL	1200	30 mM $NaClO_4$	$1.7 (\pm 0.02)\times10^{-2}$	fluence-based first order	271	>542	
tetA	1191	plasmid	pEB1-tetA	extracellular	4865	*E. coli* DH10B	gene damage (by qPCR)	8×10^8 copies/µL	216	30 mM $NaClO_4$	$2.8 (\pm 0.03)\times10^{-3}$	fluence-based first order	1645	>3000	
sul1	840	plasmid	pEB1-sul1	intracellular	4514	*E. coli* DH10B	gene damage (by qPCR)	~$2.8e\times10^7$ CFU/mL	827	30 mM $NaClO_4$	$1.2 (\pm 0.02)\times10^{-2}$	fluence-based first order	384	~600	
sul1	840	plasmid	pEB1-sul1	intracellular	4514	*E. coli* DH10B	gene damage (by qPCR)	~$2.8e\times10^7$ CFU/mL	162	30 mM $NaClO_4$	$2.3 (\pm 0.02)\times10^{-3}$	fluence-based first order	2003	>3000	
sul1	840	plasmid	pEB1-sul1	extracellular	4514	*E. coli* DH10B	gene damage (by qPCR)	$1.3e\times10^9$ copies/µL	827	30 mM $NaClO_4$	$1.6 (\pm 0.05)\times10^{-2}$	fluence-based first order	288	~1500	
sul1	840	plasmid	pEB1-sul1	extracellular	4514	*E. coli* DH10B	gene damage (by qPCR)	1.3×10^9 copies/µL	162	30 mM $NaClO_4$	$2.8 (\pm 0.02)\times10^{-3}$	fluence-based first order	1645	>3000	
ampR	861	plasmid	pUC19	extracellular	2686	*E. coli* DH5α	gene damage (by qPCR)	1 µg/mL	192	2 mM PBS; pH 7	$2.0 (\pm 0.05)\times10^{-2}$	fluence-based first order	N.A.	N.A.	Nihemaiti *et al.*, 2020 [10]
ampR	861	plasmid	pUC19	extracellular	2686	*E. coli* DH5α	gene damage (by qPCR)	1 µg/mL	400	2 mM PBS; pH 7	$3.4 (\pm 0.07)\times10^{-2}$	fluence-based first order	135	N.A.	
ampR	861	plasmid	pUC19	extracellular	2686	*E. coli* DH5α	gene damage (by qPCR)	1 µg/mL	603	2 mM PBS; pH 7	$5.8 (\pm 0.11)\times10^{-2}$	fluence-based first order	79	N.A.	
ampR	861	plasmid	pUC19	extracellular	2686	*E. coli* DH5α	gene damage (by qPCR)	1 µg/mL	851	2 mM PBS; pH 7	$8.9 (\pm 0.16)\times10^{-2}$	fluence-based first order	52	104	
ampR	861	plasmid	pUC19	extracellular	2686	*E. coli* DH5α	transformation activity	1 µg/mL		2 mM PBS; pH 7	$6.5 (\pm 0.21)\times10^{-2}$	fluence-based first order	71	N.A.	
ampR	861	plasmid	pUC19	extracellular	2686	*E. coli* DH5α	transformation activity	1 µg/mL		2 mM PBS; pH 7	$1.0 (\pm 0.03)\times10^{-1}$	fluence-based first order	46	92	
ampR	861	plasmid	pUC19	extracellular	2686	*E. coli* DH5α	transformation activity	1 µg/mL		2 mM PBS; pH 7	$2.4 (\pm 0.06)\times10^{-1}$	fluence-based first order	19	38	

ampR	861	plasmid	pUC19	extracellular	2686	*E. coli* DH5α	transformation activity	1 μg/mL		2 mM PBS; pH 7	1.6 (± 0.06)×10^{-1}	fluence-based first order	29	N.A.	
ampR	861	plasmid	pUC19	extracellular	2686	*E. coli* DH5α	transformation activity	1 μg/mL		2 mM PBS; pH 7	N.A. (too fast)				
sul1	840			intracellular		*Pseudomonas* HLS-6	gene damage (by qPCR)	1×10^{6} CFU/mL	162	PBS; pH 7	1.96×10^{-2}	fluence-based first order	235	N.A.	Zhang *et al.*, 2019 [11]
intI1				intracellular		*Pseudomonas* HLS-6	gene damage (by qPCR)	~1×10^{6} CFU/mL	146	PBS; pH 7	2.99×10^{-2}	fluence-based first order	154	N.A.	
blt		chromosome		extracellular			gene damage (by qPCR)	1 ng/μL	266	10 mM PBS;pH 7	2.0 (± 0.1) ×10^{-2}	fluence-based first order	> 88 (0.6-$\log_{10}$)	N.A.	He *et al.*, 2019 [12]
blt		chromosome		extracellular			gene damage (by qPCR)	1 ng/μL	832	10 mM PBS;pH 7	5.2 (± 0.2) ×10^{-2}	fluence-based first order	> 88(1.6-$\log_{10}$)	N.A.	
blt		chromosome		extracellular			gene damage (by qPCR)	1 ng/μL	870	10 mM PBS pH 7	7.8 (± 0.4) ×10^{-2}	fluence-based first order	66	N.A.	
blt		chromosome		extracellular			gene damage (by qPCR)	1 ng/μL	1017	10 mM PBS;pH 7	8.8 (± 0.4) ×10^{-2}	fluence-based first order	53	N.A.	
blt		chromosome		extracellular		*Bacillus subtilis* 1A189	transformation activity	1 ng/μL		10 mM PBS;pH 7			109	N.A.	
blt		chromosome		intracellular		*Bacillus subtilis* 1A189	transformation activity	1×10^{6} CFU/mL		10 mM PBS;pH 7			> 66 (1.9-$\log_{10}$)	N.A.	
ampR	860	plasmid	pUC19	extracellular	2686	*E. coli* DH5α	gene damage (by qPCR)	~1×10^{11} copies/mL	192	2 mM PBS; pH 7	1.9 (± 0.11) ×10^{-2}	fluence-based first order			Yoon *et al.*, 2018 [13]
ampR	860	plasmid	pUC19	extracellular	2686	*E. coli* DH5α	gene damage (by qPCR)	~1×10^{11} copies/mL	400	2 mM PBS; pH 7	3.1 (± 0.09) ×10^{-2}	fluence-based first order			
ampR	860	plasmid	pUC19	extracellular	2686	*E. coli* DH5α	gene damage (by qPCR)	~1×10^{11} copies/mL	603	2 mM PBS; pH 7	5.4 (± 0.16) ×10^{-2}	fluence-based first order			
ampR	860	plasmid	pUC19	extracellular	2686	*E. coli* DH5α	gene damage (by qPCR)	~1×10^{11} copies/mL	851	2 mM PBS; pH 7	1.0 (± 0.03) ×10^{-1}	fluence-based first order			
ampR	860	plasmid	pUC19	extracellular	2686	*E. coli* DH5α	transformation activity	~1×10^{11} copies/mL		2 mM PBS; pH 7	6.1 (± 0.30)×10^{-2}	fluence-based first order	76	151	
ampR	860	plasmid	pUC19	intracellular	2686	*E. coli* DH5α	gene damage (by qPCR)	~5×10^{6} CFU/mL	192	2 mM PBS; pH 7	1.7 (± 0.09)×10^{-2}	fluence-based first order			
ampR	860	plasmid	pUC19	intracellular	2686	*E. coli* DH5α	gene damage (by qPCR)	~5×10^{6} CFU/mL	400	2 mM PBS; pH 7	2.8 (± 0.06)×10^{-2}	fluence-based first order			
ampR	860	plasmid	pUC19	intracellular	2686	*E. coli* DH5α	gene damage (by qPCR)	~5×10^{6} CFU/mL	603	2 mM PBS; pH 7	4.6 (± 0.18)×10^{-2}	fluence-based first order			
ampR	860	plasmid	pUC19	intracellular	2686	*E. coli* DH5α	gene damage (by qPCR)	~5×10^{6} CFU/mL	851	2 mM PBS; pH 7	7.2 (± 0.35)×10^{-2}	fluence-based first order			
ori	589	plasmid	pUC19	extracellular	2686	*E. coli* DH5α	gene damage (by qPCR)	~1×10^{11} copies/mL	190	2 mM PBS; pH 7	1.7 (± 0.09)×10^{-2}	fluence-based first order			
ori	589	plasmid	pUC19	extracellular	2686	*E. coli* DH5α	gene damage (by qPCR)	~1×10^{11} copies/mL	390	2 mM PBS; pH 7	2.9 (± 0.12) ×10^{-2}	fluence-based first order			
ori	589	plasmid	pUC19	extracellular	2686	*E. coli* DH5α	gene damage (by qPCR)	~1×10^{11} copies/mL	530	2 mM PBS; pH 7	4.0 (± 0.24) ×10^{-2}	fluence-based first order			
ori	589	plasmid	pUC19	intracellular	2686	*E. coli* DH5α	transformation activity	~5×10^{6} CFU/mL		2 mM PBS; pH 7	6.2 (± 0.4) ×10^{-2}	fluence-based first order	74	151	

ampR	860	plasmid	pUC4k	extracellular	3914	*E. coli* DH5*α*	gene damage (by qPCR)	~1×10^{10} copies/mL	850	2 mM PBS; pH 7	1.1 (± 0.01) $\times10^{-1}$	fluence-based first order	42	84	Yoon *et al.*, 2017 [14]
kanR	815	plasmid	pUC4k	extracellular	3914	*E. coli* DH5*α*	gene damage (by qPCR)	~1×10^{10} copies/mL	806	2 mM PBS; pH 7	1.5 (± 0.06) $\times10^{-1}$	fluence-based first order	31	61	
ampR	860	plasmid	pUC4k	intracellular	3914	*E. coli* DH5*α*	gene damage (by qPCR)	~5×10^{5} CFU/mL	850	2 mM PBS; pH 7	7.0 (± 0.3) $\times10^{-2}$	fluence-based first order	66	132	
kanR	815	plasmid	pUC4k	intracellular	3914	*E. coli* DH5*α*	gene damage (by qPCR)	~5×10^{5} CFU/mL	806	2 mM PBS; pH 7	9.0 (± 1.4) $\times10^{-2}$	fluence-based first order	51	102	
ampR	860	plasmid	pUC4k	extracellular	3914	*E. coli* DH5*α*	gene damage (by qPCR)	~1×10^{10} copies/mL	850	2 mM PBS; pH 8	1.0 (± 0.06) $\times10^{-1}$	fluence-based first order	46	92	
kanR	815	plasmid	pUC4k	extracellular	3914	*E. coli* DH5*α*	gene damage (by qPCR)	~1×10^{10} copies/mL	806	2 mM PBS; pH 8	1.3 (± 0.1)$\times10^{-1}$	fluence-based first order	35	71	
ampR	860	plasmid	pUC4k	intracellular	3914	*E. coli* DH5*α*	gene damage (by qPCR)	~5×10^{5} CFU/mL	850	2 mM PBS; pH 8	6.5 (± 0.9) $\times10^{-2}$	fluence-based first order	71	142	
kanR	815	plasmid	pUC4k	intracellular	3914	*E. coli* DH5*α*	gene damage (by qPCR)	~5×10^{5} CFU/mL	806	2 mM PBS; pH 8	7.2 (± 0.9)$\times10^{-2}$	fluence-based first order	64	128	
ampR and *kanR*						*E. coli* DH5*α*	Culturability (selective agar)	~5×10^{5} CFU/mL		2 mM PBS; pH 7	2.1 (± 0.1)	fluence-based first order	2.2	4.4	
ampR	860	plasmid	pUC4k	extracellular	3914	*E. coli* DH5*α*	gene damage (by qPCR)	~1×10^{10} copies/mL	850	Spiked municiple wastewater effluent (activated sludge); pH 7	1.1×10^{-1}	fluence-based first order	42	< LOQ	
kanR	815	plasmid	pUC4k	extracellular	3914	*E. coli* DH5*α*	gene damage (by qPCR)	~1×10^{10} copies/mL	806	spiked municiple wastewater effluent (activated sludge); pH 7	9.5×10^{-2}	fluence-based first order	31	< LOQ	
ampR	860	plasmid	pUC4k	intracellular	3914	*E. coli* DH5*α*	gene damage (by qPCR)	~5×10^{5} CFU/mL	850	spiked municiple wastewater effluent (activated sludge); pH 7	6.2×10^{-2}	fluence-based first order	66	< LOQ	
kanR	815	plasmid	pUC4k	intracellular	3914	*E. coli* DH5*α*	gene damage (by qPCR)	~5×10^{5} CFU/mL	806	spiked municiple wastewater effluent (activated sludge); pH 7	6.3×10^{-2}	fluence-based first order	51	< LOQ	
tetA	1191	plasmid	pWH1266	extracellular		*E. coli* TOP10	gene damage (by qPCR)	10 ng/μL	1200	DNase free water	5.8 (± 0.6)$\times10^{-2}$	fluence-based first order	> 108 (1.7-$\log_{10}$)	N.A.	Chang *et al.*, 2017 [7]
tetA	1191	plasmid	pWH1266	extracellular		*E. coli* TOP10	gene damage (by qPCR)	10 ng/μL	216	DNase free water	4.0 (± 0.5)$\times10^{-3}$	fluence-based first order	> 430 (0.75-$\log_{10}$)	N.A.	
tetA	1191	plasmid	pWH1266	extracellular		*E. coli* TOP10	ARG transformation activity	10 ng/μL		DNase free water	1.02 (± 0.19)$\times10^{-1}$	fluence-based first order	45	N.A.	
*bla*TEM-1	861	plasmid	pWH1266	extracellular		*E. coli* TOP10	gene damage (by qPCR)	10 ng/μL	861	DNase free water	6.8 (± 0.4)$\times10^{-2}$	fluence-based first order	68	N.A.	
*bla*TEM-1	861	plasmid	pWH1266	extracellular		*E. coli* TOP10	gene damage (by qPCR)	10 ng/μL	209	DNase free water	5.5 (± 0.6)$\times10^{-3}$	fluence-based first order	> 430 (1-$\log_{10}$)	N.A.	
*bla*TEM-1	861	plasmid	pWH1266	extracellular		*E. coli* TOP10	transformation activity	10 ng/μL		DNase free water	1.13 (± 0.09)$\times10^{-1}$	fluence-based first order	40	N.A.	
ampC		chromosome	Unkown	extracellular		multiantibiotic-resistant *Pseudomonas aeruginosa* 01	gene damage (by qPCR)	1×10^{4}- 1×10^{7} copies/μL	1006	Nanopure water	N.A.		~180	N.A.	Mckinney *et al.*, 2012 11,30[1] [5]

mecA		chromosome	Type IV staphylococcal chromosomal cassette mec	extracellular		methicillin-resistant *Staphylococcus aureus* (MRSA)	gene damage (by qPCR)	1×10^4- 1×10^7 copies/µL	1018	Nanopure water	N.A.		~70	N.A.	
tetA		plasmid	pSMS35_130	extracellular		multiantibiotic-resistant *E. coli* SMS-3-5	gene damage (by qPCR)	1×10^4- 1×10^7 copies/µL	1054	Nanopure water	N.A.		~180	N.A.	
vanA		chromosome or plasmid		extracellular		vancomycin-resistant *Enterococcus faecium*	gene damage (by qPCR)	1×10^4- 1×10^7 copies/µL	1030	Nanopure water	N.A.		~75	N.A.	
ampC		chromosome		intracellular		multiantibiotic-resistant *Pseudomonas aeruginosa* 01	gene damage (by qPCR)		1006	PBS/filtered wastewater	N.A.		~240	N.A.	
mecA		chromosome	Type IV staphylococcal chromosomal cassette mec	intracellular		methicillin-resistant *Staphylococcus aureus* (MRSA)	gene damage (by qPCR)		1018	PBS/filtered wastewater	N.A.		~70	N.A.	
tetA		plasmid	pSMS35_130	intracellular		multiantibiotic-resistant *E. coli* SMS-3-5	gene damage (by qPCR)		1054	PBS/filtered wastewater	N.A.		~200	N.A.	
vanA		chromosome or plasmid		intracellular		vancomycin-resistant *Enterococcus faecium*	gene damage (by qPCR)		1030	PBS/filtered wastewater	N.A.		~80	N.A.	
UV_{254}/H_2O_2															
$[H_2O_2]_0$=0.5 mm															
ampR	861	plasmid	pUC19	extracellular	2686	*E. coli* DH5α	gene damage (by qPCR)	0.3 µg/mL	192	2 mM PBS; pH 7	10.34 (± 0.21) $\times10^{-2}$	fluence-based first order	45	89	Nihemaiti *et al.*, 2020 [10]
ampR	861	plasmid	pUC19	extracellular	2686	*E. coli* DH5α	gene damage (by qPCR)	0.3 µg/mL	400	2 mM PBS; pH 7	14.81 (± 0.78) $\times10^{-2}$	fluence-based first order	31	N.A.	
ampR	861	plasmid	pUC19	extracellular	2686	*E. coli* DH5α	gene damage (by qPCR)	0.3 µg/mL	603	2 mM PBS; pH 7	19.34 (± 0.97) $\times10^{-2}$	fluence-based first order	24	48	

ampR	861	plasmid	pUC19	extracellular	2686	*E. coli* DH5α	gene damage (by qPCR)	0.3 μg/mL	851	2 mM PBS; pH 7	29.99 (± 2.10) ×10^{-2}	fluence-based first order	15	31		
ampR	861	plasmid	pUC19	extracellular	2686	*E. coli* DH5α	transformation activity	0.3 μg/mL		2 mM PBS; pH 7	5.11 (± 0.18) ×10^{-2}	fluence-based first order	90	~180		
[[H_2O_2]$_0$=10 mg/L																
ampR	860	plasmid	pUC19	extracellular	2686	*E. coli* DH5α	gene damage (by qPCR)	~1×10^{11} copies/mL	192	2 mM PBS; pH 7	2.5 (± 0.14) ×10^{-2}	fluence-based first order			Yoon *et al.*, 2018 [13]	
ampR	860	plasmid	pUC19	extracellular	2686	*E. coli* DH5α	gene damage (by qPCR)	~1×10^{11} copies/mL	400	2 mM PBS; pH 7	4.1 (± 0.16) ×10^{-2}	fluence-based first order				
ampR	860	plasmid	pUC19	extracellular	2686	*E. coli* DH5α	gene damage (by qPCR)	~1×10^{11} copies/mL	603	2 mM PBS; pH 7	6.7 (± 0.28) ×10^{-2}	fluence-based first order				
ampR	860	plasmid	pUC19	extracellular	2686	*E. coli* DH5α	gene damage (by qPCR)	~1×10^{11} copies/mL	851	2 mM PBS; pH 7	1.8 (± 0.06) ×10^{-1}	fluence-based first order				
ampR	860	plasmid	pUC19	extracellular	2686	*E. coli* DH5α	transformation activity	~1×10^{11} copies/mL		2 mM PBS; pH 7	7.3 (± 0.4) ×10^{-2}	fluence-based first order	63	126		
ampR	860	plasmid	pUC19	intracellular	2686	*E. coli* DH5α	gene damage (by qPCR)	~5×10^{6} CFU/mL	192	2 mM PBS; pH 7	1.6 (± 0.09)×10^{-2}	fluence-based first order				
ampR	860	plasmid	pUC19	intracellular	2686	*E. coli* DH5α	gene damage (by qPCR)	~5×10^{6} CFU/mL	400	2 mM PBS; pH 7	2.9 (± 0.12) ×10^{-2}	fluence-based first order				
ampR	860	plasmid	pUC19	intracellular	2686	*E. coli* DH5α	gene damage (by qPCR)	~5×10^{6} CFU/mL	603	2 mM PBS; pH 7	4.8 (± 0.28) ×10^{-2}	fluence-based first order				
ampR	860	plasmid	pUC19	intracellular	2686	*E. coli* DH5α	gene damage (by qPCR)	~5×10^{6} CFU/mL	851	2 mM PBS; pH 7	7.3 (± 0.30) ×10^{-2}	fluence-based first order				
ori	589	plasmid	pUC19	extracellular	2686	*E. coli* DH5α	gene damage (by qPCR)	~1×10^{11} copies/mL	190	2 mM PBS; pH 7	2.3 (± 0.05) ×10^{-2}	fluence-based first order				
ori	589	plasmid	pUC19	extracellular	2686	*E. coli* DH5α	gene damage (by qPCR)	~1×10^{11} copies/mL	390	2 mM PBS; pH 7	3.9 (± 0.14) ×10^{-2}	fluence-based first order				
ori	589	plasmid	pUC19	extracellular	2686	*E. coli* DH5α	gene damage (by qPCR)	~1×10^{11} copies/mL	530	2 mM PBS; pH 7	4.7 (± 0.21) ×10^{-2}	fluence-based first order				
ori	589	plasmid	pUC19	intracellular	2686	*E. coli* DH5α	transformation activity	~5×10^{6} CFU/mL		2 mM PBS; pH 7	6.4 (± 0.4) ×10^{-2}	fluence-based first order	72	144		
[H_2O_2]$_0$==10 mg/L																
ampR	860	plasmid	pUC4k	extracellular	3914	*E. coli* DH5α	gene damage (by qPCR)	~1×10^{10} copies/mL	850	2 mM PBS; pH 7	2.1 (± 0.2) ×10^{-1}	fluence-based first order	22	44	Yoon *et al.*, 2017 [14]	
kanR	815	plasmid	pUC4k	extracellular	3914	*E. coli* DH5α	gene damage (by qPCR)	~1×10^{10} copies/mL	806	2 mM PBS; pH 7	2.1 (± 0.3) ×10^{-1}	fluence-based first order	22	44		
ampR	860	plasmid	pUC4k	intracellular	3914	*E. coli* DH5α	gene damage (by qPCR)	~5×10^{5} CFU/mL	850	2 mM PBS; pH 7	6.3 (± 0.6) ×10^{-2}	fluence-based first order	73	146		
kanR	815	plasmid	pUC4k	intracellular	3914	*E. coli* DH5α	gene damage (by qPCR)	~5×10^{5} CFU/mL	806	2 mM PBS; pH 7	7.1 (± 0.3) ×10^{-2}	fluence-based first order	65	130		
ampR	860	plasmid	pUC4k	extracellular	3914	*E. coli* DH5α	gene damage (by qPCR)	~1×10^{10} copies/mL	850	2 mM PBS; pH 8	1.3 (± 0.4) ×10^{-1}	fluence-based first order	35	71		
kanR	815	plasmid	pUC4k	extracellular	3914	*E. coli* DH5α	gene damage (by qPCR)	~1×10^{10} copies/mL	806	2 mM PBS; pH 8	2.0 (± 0.2) ×10^{-1}	fluence-based first order	23	46		
ampR	860	plasmid	pUC4k	intracellular	3914	*E. coli* DH5α	gene damage (by qPCR)	~5×10^{5} CFU/mL	850	2 mM PBS; pH 8	7.0 (± 3.5) ×10^{-2}	fluence-based first order	66	132		
kanR	815	plasmid	pUC4k	intracellular	3914	*E. coli* DH5α	gene damage (by qPCR)	~5×10^{5} CFU/mL	806	2 mM PBS; pH 8	8.8 (± 0.6) ×10^{-2}	fluence-based first order	52	105		
ampR and *kanR*						*E. coli* DH5α	culturability (selective agar)	~5×10^{5} CFU/mL		2 mM PBS; pH 7	2.2 (± 0.1)	fluence-based first order	2.1	4.2		

ampR	860	plasmid	pUC4k	extracellular	3914	*E. coli* DH5α	gene damage (by qPCR)	~1×10^{10} copies/mL	850	spiked municiple wastewater effluent (activated sludge); pH 7	1.1×10^{-1}	fluence-based first order	42	< LOQ	
kanR	815	plasmid	pUC4k	extracellular	3914	*E. coli* DH5α	gene damage (by qPCR)	~1×10^{10} copies/mL	806	spiked municiple wastewater effluent (activated sludge); pH 7	1.0×10^{-1}	fluence-based first order	46	< LOQ	
ampR	860	plasmid	pUC4k	intracellular	3914	*E. coli* DH5α	gene damage (by qPCR)	~5×10^{5} CFU/mL	850	spiked municiple wastewater effluent (activated sludge); pH 7	5.4×10^{-2}	fluence-based first order	85	< LOQ	
kanR	815	plasmid	pUC4k	intracellular	3914	*E. coli* DH5α	gene damage (by qPCR)	~5×10^{5} CFU/mL	806	spiked municiple wastewater effluent (activated sludge); pH 7	6.2×10^{-2}	fluence-based first order	74	< LOQ	
$UV_{254}/S_2O_8^{2-}$															
$[S_2O_8^{2-}]_0$=0.5 mM															
ampR	861	plasmid	pUC19	extracellular	2686	*E. coli* DH5α	gene damage (by qPCR)	0.3 μg/mL	192	2 mM PBS; pH 7	$10.50 (\pm 0.48)\times10^{-2}$	fluence-based first order	44	N.A.	Nihemaiti *et al.*, 2020 [10]
ampR	861	plasmid	pUC19	extracellular	2686	*E. coli* DH5α	gene damage (by qPCR)	0.3 μg/mL	400	2 mM PBS; pH 7	$17.09 (\pm 0.46)\times10^{-2}$	fluence-based first order	27	54	
ampR	861	plasmid	pUC19	extracellular	2686	*E. coli* DH5α	gene damage (by qPCR)	0.3 μg/mL	603	2 mM PBS; pH 7	$22.87 (\pm 1.57)\times10^{-2}$	fluence-based first order	24	48	
ampR	861	plasmid	pUC19	extracellular	2686	*E. coli* DH5α	gene damage (by qPCR)	0.3 μg/mL	851	2 mM PBS; pH 7	$31.85 (\pm 1.57)\times10^{-2}$	fluence-based first order	14	29	
ampR	861	plasmid	pUC19	extracellular	2686	*E. coli* DH5α	transformation activity	0.3 μg/mL		2 mM PBS; pH 7	$5.16 (\pm 0.09)\times10^{-2}$	fluence-based first order	89	179	
UV_{254}/Cl_2															
$[Cl_2]_0$=20 mg/L															
sul1				intracellular		*Pseudomonas* HLS-6	gene damage (by qPCR)	~1×10^{6} CFU/mL	162	PBS; pH 7	1.27×10^{-1}	first order	36	N.A.	Zhang *et al.*, 2019 [11]
intl1				intracellular		*Pseudomonas* HLS-6	gene damage (by qPCR)	~1×10^{6} CFU/mL	146	PBS; pH 7	1.42×10^{-1}	first order	33	N.A.	
UV_{254} assisted electrochemistry															
30 mA of DC															
tetA	1191	plasmid	pEB1-tetA		4865	*E. coli* DH10B	culturability (selective agar)	~2.3×10^{7} CFU/mL		30 mM $NaClO_4$				50 (4.1-$\log_{10}$)	This study
sul1	840	plasmid	pEB1-sul1		4514	*E. coli* DH10B	culturability (selective agar)	~2.8×10^{7} CFU/mL		30 mM $NaClO_4$				50 (4.0-$\log_{10}$)	
tetA	1191	plasmid	pEB1-tetA	intracellular	4865	*E. coli* DH10B	gene damage (by qPCR)	~2.3×10^{7} CFU/mL	1200	30 mM $NaClO_4$	$2.0 (\pm 0.05)\times10^{-2}$	fluence-based first order	230	1500 (4.0-$\log_{10}$)	
tetA	1191	plasmid	pEB1-tetA	intracellular	4865	*E. coli* DH10B	gene damage (by qPCR)	~2.3×10^{7} CFU/mL	216	30 mM $NaClO_4$	$3.0 (\pm 0.03)\times10^{-3}$	fluence-based first order	1535	3000 (3.8-$\log_{10}$)	
tetA	1191	plasmid	pEB1-tetA	extracellular	4865	*E. coli* DH10B	gene damage (by qPCR)	8×10^{8} copies/μL	1200	30 mM $NaClO_4$	$2.6 (\pm 0.07)\times10^{-2}$	fluence-based first order	177	600 (4.6-$\log_{10}$)	

tetA	1191	plasmid	pEB1-tetA	extracellular	4865	*E. coli* DH10B	gene damage (by qPCR)	8×10^{8} copies/µL	216	30 mM $NaClO_4$	3.7 (± 0.02) $\times10^{-3}$	fluence-based first order	1245	2490
sul1	840	plasmid	pEB1-sul1	intracellular	4514	*E. coli* DH10B	gene damage (by qPCR)	~$2.8e\times10^{7}$ CFU/mL	827	30 mM $NaClO_4$	1.8 (± 0.03) $\times10^{-2}$	fluence-based first order	256	1500 (5.2-$\log_{10}$)
sul1	840	plasmid	pEB1-sul1	intracellular	4514	*E. coli* DH10B	gene damage (by qPCR)	~$2.8e\times10^{7}$ CFU/mL	162	30 mM $NaClO_4$	2.6 (± 0.03) $\times10^{-3}$	fluence-based first order	1772	3000 (3.4-$\log_{10}$)
sul1	840	plasmid	pEB1-sul1	extracellular	4514	*E. coli* DH10B	gene damage (by qPCR)	$1.3e\times10^{9}$ copies/µL	827	30 mM $NaClO_4$	2.6 (± 0.03) $\times10^{-2}$	fluence-based first order	177	354
sul1	840	plasmid	pEB1-sul1	extracellular	4514	*E. coli* DH10B	gene damage (by qPCR)	1.3×10^{9} copies/µL	162	30 mM $NaClO_4$	3.5 (± 0.02) $\times10^{-3}$	fluence-based first order	1316	2632
tetA	1191	plasmid	pEB1-tetA		4865	*E. coli* DH10B	culturability (selective agar)	~2.3×10^{7} CFU/mL		30 mM NaCl		fluence-based first order		50 (4.8-$\log_{10}$)
sul1	840	plasmid	pEB1-sul1		4514	*E. coli* DH10B	culturability (selective agar)	~2.8×10^{7} CFU/mL		30 mM NaCl		fluence-based first order		50 (5.0-$\log_{10}$)
tetA	1191	plasmid	pEB1-tetA	intracellular	4865	*E. coli* DH10B	gene damage (by qPCR)	~2.3×10^{7} CFU/mL	1200	30 mM NaCl	3.0 (± 0.10)$\times10^{-2}$	fluence-based first order	154	300 (3.7-$\log_{10}$)
tetA	1191	plasmid	pEB1-tetA	intracellular	4865	*E. coli* DH10B	gene damage (by qPCR)	~2.3×10^{7} CFU/mL	216	30 mM NaCl	4.6(± 0.02) $\times10^{-3}$	fluence-based first order	1001	2003
tetA	1191	plasmid	pEB1-tetA	extracellular	4865	*E. coli* DH10B	gene damage (by qPCR)	8×10^{8} copies/µL	1200	30 mM NaCl	3.6 (± 0.03) $\times10^{-2}$	fluence-based first order	128	256
tetA	1191	plasmid	pEB1-tetA	extracellular	4865	*E. coli* DH10B	gene damage (by qPCR)	8×10^{8} copies/µL	216	30 mM NaCl	4.8 (± 0.02) $\times10^{-3}$	fluence-based first order	960	1919
sul1	840	plasmid	pEB1-sul1	intracellular	4514	*E. coli* DH10B	gene damage (by qPCR)	~2.8×10^{7}, CFU/mL	827	30 mM NaCl	2.7 (± 0.07) $\times10^{-2}$	fluence-based first order	171	300 (3.4-$\log_{10}$)
sul1	840	plasmid	pEB1-sul1	intracellular	4514	*E. coli* DH10B	gene damage (by qPCR)	~2.8×10^{7} CFU/mL	162	30 mM NaCl	3.9 (± 0.02) $\times10^{-3}$	fluence-based first order	1181	2362
sul1	840	plasmid	pEB1-sul1	extracellular	4514	*E. coli* DH10B	gene damage (by qPCR)	1.3×10^{9} copies/µL	827	30 mM NaCl	3.4 (± 0.07) $\times10^{-2}$	fluence-based first order	135	271
sul1	840	plasmid	pEB1-sul1	extracellular	4514	*E. coli* DH10B	gene damage (by qPCR)	1.3×10^{9} copies/µL	162	30 mM NaCl	4.1 (± 0.02) $\times10^{-3}$	fluence-based first order	1123	1123
						native bacteria in wastewater	culturability (non-selective agar)	~6.4×10^{3} CFU/mL		latrine wastewater			150 (1.9-$\log_{10}$)	300 (2.7-$\log_{10}$)
tetA	1191					native bacteria in wastewater	gene damage (by qPCR)	$5.8e\times10^{2}$ copies/µL	1200	latrine wastewater			600 (1.1-$\log_{10}$)	
tetA	1191					native bacteria in wastewater	gene damage (by qPCR)	$2.5e\times10^{3}$ copies/µL	216	latrine wastewater			3000 (1.9-$\log_{10}$)	
sul1	840					native bacteria in wastewater	gene damage (by qPCR)	7.5×10^{3} copies/µL	827	latrine wastewater			600 (1.9-$\log_{10}$)	
sul1	840					native bacteria in wastewater	gene damage (by qPCR)	2.2×10^{4} copies/µL	162	latrine wastewater			9000 (1.8-$\log_{10}$)	

$UV_{>290}/H_2O_2$

$[H_2O_2]_0$=10 mM

ampR	861	plasmid	pUC19	extracellular	2686	*E. coli* DH5α	gene damage (by qPCR)	1 μg/mL	192	2 mM PBS; pH 7	8.1 (± 0.69) ×10^9	fluence-based first order	N.A.	N.A.	Nihemaiti *et al.*, 2020 [10]
ampR	861	plasmid	pUC19	extracellular	2686	*E. coli* DH5α	gene damage (by qPCR)	1 μg/mL	400	2 mM PBS; pH 7	2.2 (± 0.07) ×10^{10}	fluence-based first order	N.A.	N.A.	
ampR	861	plasmid	pUC19	extracellular	2686	*E. coli* DH5α	gene damage (by qPCR)	1 μg/mL	603	2 mM PBS; pH 7	3.5 (± 0.10) ×10^{10}	fluence-based first order	1.32×10^{-10}	N.A.	
ampR	861	plasmid	pUC19	extracellular	2686	*E. coli* DH5α	gene damage (by qPCR)	1 μg/mL	851	2 mM PBS; pH 7	5.6 (± 0.27) ×10^{10}	fluence-based first order	8.23×10^{-11}	1.65×10^{-10}	
ampR	861	plasmid	pUC19	extracellular	2686	*E. coli* DH5α	transformation activity	1 μg/mL		2 mM PBS; pH 7	2.7 (± 0.05) ×10^{10}	fluence-based first order	1.71×10^{-10}	N.A.	
ampR	861	plasmid	pUC19	extracellular	2686	*E. coli* AB1157	transformation activity	1 μg/mL		2 mM PBS; pH 7	4.1 (± 0.14) ×10^{10}	fluence-based first order	1.12×10^{-10}	N.A.	
ampR	861	plasmid	pUC19	extracellular	2686	*E. coli* AB1886	transformation activity	1 μg/mL		2 mM PBS; pH 7	6.5 (± 0.18) ×10^{10}	fluence-based first order	7.09×10^{-11}	N.A.	
ampR	861	plasmid	pUC19	extracellular	2686	*E. coli* AB2463	transformation activity	1 μg/mL		2 mM PBS; pH 7	8.2 (± 0.23) ×10^{10}	fluence-based first order	5.62×10^{-11}	N.A.	
ampR	861	plasmid	pUC19	extracellular	2686	*E. coli* AB2480	transformation activity	1 μg/mL		2 mM PBS; pH 7	N.A. (too fast)				
blt		chromosome		extracellular			gene damage (by qPCR)	1 ng/μL	266	10 mM PBS;pH 7	5.9 (± 0.8) ×10^{10}	second order	> 2.6 × 10^{-11}(0.8-$\log_{10}$)		He *et al.*, 2019 [12]
blt		chromosome		extracellular			gene damage (by qPCR)	1 ng/μL	832	10 mM PBS;pH 7	1.9 (± 0.2) ×10^{11}	second order	2.1×10^{-11}		
blt		chromosome		extracellular			gene damage (by qPCR)	1 ng/μL	870	10 mM PBSpH 7	2.0 (± 0.2) ×10^{11}	second order	2.1 ×10^{-11}		
blt		chromosome		extracellular			gene damage (by qPCR)	1 ng/μL	1017	10 mM PBS;pH 7	2.3 (± 0.3) ×10^{11}	second order	1.8×10^{-11}		
blt		chromosome		extracellular		*Bacillus subtilis* 1A189	transformation activity	1 ng/μL		10 mM PBS;pH 7			> 6.5 ×10^{-12} (1.7-$\log_{10}$)		
				intracellular		*Bacillus subtilis* 1A189	culturability	1×10^6 CFU/mL		10 mM PBS; pH 7					
				intracellular		*Bacillus subtilis* 1A189	transformation activity	1×10^6 CFU/mL		10 mM PBS; pH 7			> 66 (1.9-$\log_{10}$)		

Chlorine

$[Cl_2]_0$=20 mg/L

sul1				intracellular		*Pseudomonas* HLS-6	gene damage (by qPCR)	~1×10^6 CFU/mL	162	PBS; pH 7	4.08×10^{-2}	first order	38	N.A.	Zhang *et al.*, 2019 [11]
intl1				intracellular		*Pseudomonas* HLS-6	gene damage (by qPCR)	~1×10^6 CFU/mL	146	PBS; pH 7	5.67×10^{-2}	first order	27	N.A.	
blt		chromosome		extracellular			gene damage (by qPCR)	1 ng/μL	266	NaOCl; pH 7	3.3 (± 0.3)	second order	100	N.A.	He *et al.*, 2019 [12]

blt		chromosome		extracellular			gene damage (by qPCR)	1 ng/μL	832	NaOCl; pH 7	7.1 (± 0.4)	second order	70	N.A.	
blt		chromosome		extracellular			gene damage (by qPCR)	1 ng/μL	870	NaOCl; pH 7	6.8 (± 0.4)	second order	67	N.A.	
blt		chromosome		extracellular			gene damage (by qPCR)	1 ng/μL	1017	NaOCl; pH 7	7.7 (± 0.4)	second order	65	N.A.	
blt		chromosome		extracellular		*Bacillus subtilis* 1A189	transformation activity	1 ng/μL		NaOCl; pH 7			> 60 (1.5-$\log_{10}$)	N.A.	
blt		chromosome		intracellular		*Bacillus subtilis* 1A189	transformation activity	1×10^{6} CFU/mL		NaOCl; pH 7			> 46 (1-$\log_{10}$)	N.A.	
$[Cl_2]_0$=5 mg/L															
ampR	860	plasmid	pUC4k	extracellular	3914	*E. coli* DH5α	gene damage (by qPCR)	~1×10^{10} copies/mL	850	2 mM PBS; pH 7	2.1 (± 0.2) $\times10^{-1}$	fluence-based first order	22	37	Yoon *et al.*, 2017 [14]
kanR	815	plasmid	pUC4k	extracellular	3914	*E. coli* DH5α	gene damage (by qPCR)	~1×10^{10} copies/mL	806	2 mM PBS; pH 7	3.1 (± 0.2) $\times10^{-1}$	fluence-based first order	28	50	
ampR	860	plasmid	pUC4k	intracellular	3914	*E. coli* DH5α	gene damage (by qPCR)	~5×10^{5} CFU/mL	850	2 mM PBS; pH 7	1.0 (± 0.1) $\times10^{-1}$	fluence-based first order	21	67	
kanR	815	plasmid	pUC4k	intracellular	3914	*E. coli* DH5α	gene damage (by qPCR)	~5×10^{5} CFU/mL	806	2 mM PBS; pH 7	1.0 (± 0.1) $\times10^{-1}$	fluence-based first order	26	72	
ampR	860	plasmid	pUC4k	extracellular	3914	*E. coli* DH5α	gene damage (by qPCR)	~1×10^{10} copies/mL	850	2 mM PBS; pH 8	7.4 (± 0.1) $\times10^{-2}$	fluence-based first order	89	152	
kanR	815	plasmid	pUC4k	extracellular	3914	*E. coli* DH5α	gene damage (by qPCR)	~1×10^{10} copies/mL	806	2 mM PBS; pH 8	2.7 (± 0.2) $\times10^{-2}$	fluence-based first order	205	376	
ampR	860	plasmid	pUC4k	intracellular	3914	*E. coli* DH5α	gene damage (by qPCR)	~5×10^{5} CFU/mL	850	2 mM PBS; pH 8	9.0 (± 0.7) $\times10^{-2}$	fluence-based first order	41	92	
kanR	815	plasmid	pUC4k	intracellular	3914	*E. coli* DH5α	gene damage (by qPCR)	~5×10^{5} CFU/mL	806	2 mM PBS; pH 8	1.0 (± 0.2) $\times10^{-1}$	fluence-based first order	35	81	
ampR and *kanR*		plasmid	pUC4k			*E. coli* DH5α	culturability (selective agar)	~5×10^{5} CFU/mL		2 mM PBS; pH 7	8.7 (± 0.9)	fluence-based first order	0.05	0.11	
ampR	860	plasmid	pUC4k	extracellular	3914	*E. coli* DH5α	gene damage (by qPCR)	~1×10^{10} copies/mL	850	municiple wastewater effluent; pH 7	~300	fluence-based first order		Generally, 20 mg/L of chlorine dose was required (1 h duration)	
kanR	815	plasmid	pUC4k	extracellular	3914	*E. coli* DH5α	gene damage (by qPCR)	~1×10^{10} copies/mL	806	municiple wastewater effluent; pH 7	~300	fluence-based first order		Generally, 20 mg/L of chlorine dose was required (1 h duration)	
ampR	860	plasmid	pUC4k	intracellular	3914	*E. coli* DH5α	gene damage (by qPCR)	~5×10^{5} CFU/mL	850	municiple wastewater effluent; pH 7	~120	fluence-based first order		Generally, 20 mg/L of chlorine dose was required (1 h duration)	
kanR	815	plasmid	pUC4k	intracellular	3914	*E. coli* DH5α	gene damage (by qPCR)	~5×10^{5} CFU/mL	806	municiple wastewater effluent; pH 7	~120	fluence-based first order		Generally, 20 mg/L of chlorine dose was required (1 h duration)	

* When the required dose for 2-$\log_{10}$ or 4-$\log_{10}$ removal falls off the linear regression data range, the data most nearby is reported.

Table S5. Mutations in pEB1-tetA detected by Sanger sequencing.

Position in pEB1-tetA	Position in *tetA* gene	Mutation	Amino acid mutation in pEB1-tetA
1230	1049	C → T	Threonine (350)→Isoleucine
1299	1118	T → C	Valine (373)→Alanine
1306	1125	C → T	Alanine (375)→Alanine
1312	1131	A → C	Leucine (377)-Leucine
1316	1135	C → -	Leucine (379)-Leucine
1320	1139	- →C	Valine (380)→Leucine
1327	1146	C → G	Leucine (382)→Leucine
1330	1149	C → G	Proline (383)-Proline

References

(1) Yang, Y.; Hoffmann, M. R. Synthesis and Stabilization of Blue-Black TiO_2 Nanotube Arrays for Electrochemical Oxidant Generation and Wastewater Treatment. *Environ. Sci. Technol.* **2016**, *50* (21), 11888–11894. https://doi.org/10.1021/acs.est.6b03540.

(2) Yang, Y.; Kao, L. C.; Liu, Y.; Sun, K.; Yu, H.; Guo, J.; Liou, S. Y. H.; Hoffmann, M. R. Cobalt-Doped Black TiO2 Nanotube Array as a Stable Anode for Oxygen Evolution and Electrochemical Wastewater Treatment. *ACS Catal.* **2018**, *8* (5), 4278–4287. https://doi.org/10.1021/acscatal.7b04340.

(3) Koo, M. S.; Cho, K.; Yoon, J.; Choi, W. Photoelectrochemical Degradation of Organic Compounds Coupled with Molecular Hydrogen Generation Using Electrochromic TiO2 Nanotube Arrays. *Environ. Sci. Technol.* **2017**, *51* (11), 6590–6598. https://doi.org/10.1021/acs.est.7b00774.

(4) Linsebigler, A. L.; Lu, Guangquan.; Yates, J. T. Photocatalysis on TiO2 Surfaces: Principles, Mechanisms, and Selected Results. *Chem. Rev.* **1995**, *95* (3), 735–758. https://doi.org/10.1021/cr00035a013.

(5) Hoffmann, M. R.; Martin, S. T.; Choi, Wonyong.; Bahnemann, D. W. Environmental Applications of Semiconductor Photocatalysis. *Chem. Rev.* **1995**, *95* (1), 69–96. https://doi.org/10.1021/cr00033a004.

(6) Yang, Y.; Zhang, S.; Wang, S.; Zhang, K.; Wang, H.; Huang, J.; Deng, S.; Wang, B.; Wang, Y.; Yu, G. Ball Milling Synthesized MnOx as Highly Active Catalyst for Gaseous POPs Removal: Significance of Mechanochemically Induced Oxygen Vacancies. *Environ. Sci. Technol.* **2015**, *49* (7), 4473–4480. https://doi.org/10.1021/es505232f.

(7) Chang, P. H.; Juhrend, B.; Olson, T. M.; Marrs, C. F.; Wigginton, K. R. Degradation of Extracellular Antibiotic Resistance Genes with UV254 Treatment. *Environ. Sci. Technol.* **2017**, *51* (11), 6185–6192. https://doi.org/10.1021/acs.est.7b01120.

(8) Czekalski, N.; Imminger, S.; Salhi, E.; Veljkovic, M.; Kleffel, K.; Drissner, D.; Hammes, F.; Bürgmann, H.; von Gunten, U. Inactivation of Antibiotic Resistant Bacteria and Resistance Genes by Ozone: From Laboratory Experiments to Full-Scale Wastewater Treatment. *Environ. Sci. Technol.* **2016**, *50* (21), 11862–11871. https://doi.org/10.1021/acs.est.6b02640.

(9) Xu, J.; Xu, Y.; Wang, H.; Guo, C.; Qiu, H.; He, Y.; Zhang, Y.; Li, X.; Meng, W. Occurrence of Antibiotics and Antibiotic Resistance Genes in a Sewage Treatment Plant and Its Effluent-Receiving River. *Chemosphere* **2015**, *119*, 1379–1385. https://doi.org/10.1016/j.chemosphere.2014.02.040.

(10) Nihemaiti, M.; Yoon, Y.; He, H.; Dodd, M. C.; Croué, J.-P.; Lee, Y. Degradation and Deactivation of a Plasmid-Encoded Extracellular Antibiotic Resistance Gene during

Separate and Combined Exposures to UV254 and Radicals. *Water Research* **2020**, *182*, 115921. https://doi.org/10.1016/j.watres.2020.115921.

(11) Zhang, T.; Hu, Y.; Jiang, L.; Yao, S.; Lin, K.; Zhou, Y.; Cui, C. Removal of Antibiotic Resistance Genes and Control of Horizontal Transfer Risk by UV, Chlorination and UV/Chlorination Treatments of Drinking Water. *Chemical Engineering Journal* **2019**, *358*, 589–597. https://doi.org/10.1016/j.cej.2018.09.218.

(12) He, H.; Zhou, P.; Shimabuku, K. K.; Fang, X.; Li, S.; Lee, Y.; Dodd, M. C. Degradation and Deactivation of Bacterial Antibiotic Resistance Genes during Exposure to Free Chlorine, Monochloramine, Chlorine Dioxide, Ozone, Ultraviolet Light, and Hydroxyl Radical. *Environ. Sci. Technol.* **2019**, *53* (4), 2013–2026. https://doi.org/10.1021/acs.est.8b04393.

(13) Yoon, Y.; Dodd, M. C.; Lee, Y. Elimination of Transforming Activity and Gene Degradation during UV and UV/H2O2 Treatment of Plasmid-Encoded Antibiotic Resistance Genes. *Environ. Sci.: Water Res. Technol.* **2018**, *4* (9), 1239–1251. https://doi.org/10.1039/C8EW00200B.

(14) Yoon, Y.; Chung, H. J.; Wen Di, D. Y.; Dodd, M. C.; Hur, H.-G.; Lee, Y. Inactivation Efficiency of Plasmid-Encoded Antibiotic Resistance Genes during Water Treatment with Chlorine, UV, and UV/H2O2. *Water Research* **2017**, *123*, 783–793. https://doi.org/10.1016/j.watres.2017.06.056.

(15) McKinney, C. W.; Pruden, A. Ultraviolet Disinfection of Antibiotic Resistant Bacteria and Their Antibiotic Resistance Genes in Water and Wastewater. *Environ. Sci. Technol.* **2012**, *46* (24), 13393–13400. https://doi.org/10.1021/es303652q.

(16) Matthew, B. M.; Anastasio, C. A Chemical Probe Technique for the Determination of Reactive Halogen Species in Aqueous Solution: Part 1 – Bromide Solutions. *Atmospheric Chemistry and Physics* **2006**, *6* (9), 2423–2437. https://doi.org/10.5194/acp-6-2423-2006.

(17) NDRL/NIST Solution Kinetics Database https://kinetics.nist.gov/solution/ (accessed Sep 20, 2019).

(18) G. Jayson, G.; J. Parsons, B.; J. Swallow, A. Some Simple, Highly Reactive, Inorganic Chlorine Derivatives in Aqueous Solution. Their Formation Using Pulses of Radiation and Their Role in the Mechanism of the Fricke Dosimeter. *Journal of the Chemical Society, Faraday Transactions 1: Physical Chemistry in Condensed Phases* **1973**, *69* (0), 1597–1607. https://doi.org/10.1039/F19736901597.

(19) Kläning, U. K.; Wolff, T. Laser Flash Photolysis of HClO, ClO−, HBrO, and BrO− in Aqueous Solution. Reactions of Cl- and Br-Atoms. *Berichte der Bunsengesellschaft für physikalische Chemie* **1985**, *89* (3), 243–245. https://doi.org/10.1002/bbpc.19850890309.

(20) Grebel, J. E.; Pignatello, J. J.; Mitch, W. A. Effect of Halide Ions and Carbonates on Organic Contaminant Degradation by Hydroxyl Radical-Based Advanced Oxidation Processes in

Saline Waters. *Environ. Sci. Technol.* **2010**, *44* (17), 6822–6828. https://doi.org/10.1021/es1010225.

(21) Wu, D.; Wong, D.; Di Bartolo, B. Evolution of Cl−2 in Aqueous NaCl Solutions. *Journal of Photochemistry* **1980**, *14* (4), 303–310. https://doi.org/10.1016/0047-2670(80)85102-1.

(22) Park, H.; Vecitis, C. D.; Hoffmann, M. R. Electrochemical Water Splitting Coupled with Organic Compound Oxidation: The Role of Active Chlorine Species. *J. Phys. Chem. C* **2009**, *113* (18), 7935–7945. https://doi.org/10.1021/jp810331w.

(23) Wang, T. X.; Margerum, D. W. Kinetics of Reversible Chlorine Hydrolysis: Temperature Dependence and General-Acid/Base-Assisted Mechanisms. *Inorganic Chemistry* **1994**, *33* (6), 1050–1055. https://doi.org/10.1021/ic00084a014.

(24) Buxton, G. V.; Greenstock, C. L.; Helman, W. P.; Ross, A. B. Critical Review of Rate Constants for Reactions of Hydrated Electrons, Hydrogen Atoms and Hydroxyl Radicals (·OH/·O− in Aqueous Solution. *Journal of Physical and Chemical Reference Data* **1988**, *17* (2), 513–886. https://doi.org/10.1063/1.555805.

(25) Bielski, B. H. J.; Cabelli, D. E.; Arudi, R. L.; Ross, A. B. Reactivity of HO2/O−2 Radicals in Aqueous Solution. *Journal of Physical and Chemical Reference Data* **1985**, *14* (4), 1041–1100. https://doi.org/10.1063/1.555739.

(26) Connick, R. E. The Interaction of Hydrogen Peroxide and Hypochlorous Acid in Acidic Solutions Containing Chloride Ion. *Journal of the American Chemical Society* **1947**, *69* (6), 1509–1514. https://doi.org/10.1021/ja01198a074.

(27) Zehavi, D.; Rabani, J. Oxidation of Aqueous Bromide Ions by Hydroxyl Radicals. Pulse Radiolytic Investigation. *J. Phys. Chem.* **1972**, *76* (3), 312–319. https://doi.org/10.1021/j100647a006.

(28) Mártire, D. O.; Rosso, J. A.; Bertolotti, S.; Le Roux, G. C.; Braun, A. M.; Gonzalez, M. C. Kinetic Study of the Reactions of Chlorine Atoms and Cl2•- Radical Anions in Aqueous Solutions. II. Toluene, Benzoic Acid, and Chlorobenzene. *J. Phys. Chem. A* **2001**, *105* (22), 5385–5392. https://doi.org/10.1021/jp004630z.

(29) Hasegawa, K.; Neta, P. Rate Constants and Mechanisms of Reaction of Chloride (Cl2-) Radicals. *J. Phys. Chem.* **1978**, *82* (8), 854–857. https://doi.org/10.1021/j100497a003.